

Electronic structure of the trilayer cuprate superconductor $\text{Bi}_2\text{Sr}_2\text{Ca}_2\text{Cu}_3\text{O}_{10+\delta}$

D.L. Feng¹, A. Damascelli¹, K.M. Shen¹, N. Motoyama², D.H. Lu¹, H. Eisaki¹, K. Shimizu³, J.-i. Shimoyama³, K. Kishio³, N. Kaneko¹, M. Greven¹, G.D. Gu⁴, X.J. Zhou¹, C. Kim¹, F. Ronning¹, N.P. Armitage¹, Z.-X. Shen¹

¹*Department of Physics, Applied Physics, and Stanford Synchrotron Radiation Laboratory, Stanford University, Stanford, California 94305*

²*Department of Superconductivity, University of Tokyo, Tokyo, 113-8656, Japan*

³*Department of Applied Chemistry, University of Tokyo, Tokyo, 113-8656, Japan*

⁴*Physics Department, Brookhaven National Laboratory, P. O. Box 5000, Upton, New York 11973*
(November 1, 2018)

The low-energy electronic structure of the trilayer cuprate superconductor $\text{Bi}_2\text{Sr}_2\text{Ca}_2\text{Cu}_3\text{O}_{10+\delta}$ near optimal doping is investigated by angle-resolved photoemission spectroscopy. The normal state quasiparticle dispersion and Fermi surface, and the superconducting d -wave gap and coherence peak are observed and compared with those of single and bilayer systems. We find that both the superconducting gap magnitude and the relative coherence-peak intensity scale linearly with T_c for various optimally doped materials. This suggests that the higher T_c of the trilayer system should be attributed to parameters that simultaneously enhance phase stiffness and pairing strength.

PACS numbers: 71.18.+y, 74.72.Hs, 79.60.Bm

The high- T_c cuprate superconductors (HTSCs), based on the number of CuO_2 planes in the characteristic multilayer blocks, can be classified into single-layer materials [e.g., $\text{Bi}_2\text{Sr}_2\text{CuO}_{6+\delta}$ (Bi2201), $\text{HgBa}_2\text{CuO}_{4+\delta}$ (Hg1201), and $\text{La}_{2-x}\text{Sr}_x\text{CuO}_4$ (LSCO)], bilayer materials [e.g., $\text{Bi}_2\text{Sr}_2\text{CaCu}_2\text{O}_{8+\delta}$ (Bi2212), $\text{HgBa}_2\text{CaCu}_2\text{O}_{6+\delta}$ (Hg1212) and $\text{YBa}_2\text{Cu}_3\text{O}_{7-\delta}$ (Y123)], trilayer materials [e.g., $\text{Bi}_2\text{Sr}_2\text{Ca}_2\text{Cu}_3\text{O}_{10+\delta}$ (Bi2223), and $\text{HgBa}_2\text{Ca}_2\text{Cu}_3\text{O}_{8+\delta}$ (Hg1223)], and so on. This structural characteristic has a direct correlation with the superconducting properties: within each family of cuprates, the superconducting phase transition temperature (T_c) increases with the layer number (n) for $n \leq 3$, and then starts to decrease [1,2]. Taking the Bi-family of HTSCs as an example, the maximum T_c is approximately 34, 90, and 110 K for optimally doped Bi2201 ($n=1$), Bi2212 ($n=2$), and Bi2223 ($n=3$), respectively. Despite various experimental and theoretical efforts, a conclusive microscopic understanding of this evolution has not yet been reached, partly because of the lack of detailed knowledge about the electronic structure of the trilayer systems. In particular, angle-resolved photoemission spectroscopy (ARPES), one of the most direct probe of the electronic structure of HTSCs [3], has so far been limited to single and bilayer compounds. To gain further insight into the role of multiple CuO_2 planes in determining the macroscopic physical properties of the cuprates, like the value of the T_c , it is crucial to extend the investigation of the electronic structure to trilayer HTSCs, and to compare the results with those from the single and bilayer materials. Given that the Bi-based cuprates represent the HTSC family best characterized by ARPES, the trilayer system Bi2223 is the ideal candidate for such a comparative study.

In this Letter, we report the first ARPES study, to the best of our knowledge, of the electronic structure of the trilayer HTSC Bi2223, for which high quality single crys-

tals with dimensions suitable for ARPES measurements has been recently synthesized. As in the single- and bilayer materials, at nearly optimally doped Bi2223, we observed a large hole-like Fermi surface, a flat quasiparticle band near $(\pi, 0)$, d -wave pseudo and superconducting gaps, and a large superconducting peak (the so-called coherence peak in the case of Bi2212). The superconducting gap magnitude and the relative weight of the superconducting peak both increase linearly with T_c for the optimally doped Bi-based HTSCs. This indicates that the higher T_c of Bi2223 is caused by the enhancement of both pairing strength and phase stiffness, consistent with the idea that optimal doping corresponds to the intersection between phase-coherence and pairing-strength temperature scales.

Bi2223 single crystals were grown by floating-zone technique. Nearly optimally doped samples [$T_c = 108$ K, $\Delta T_c(10\% - 90\%) = 2$ K] were obtained by subsequently annealing the slightly underdoped as-grown Bi2223 crystals ($T_c = 105$ K) for three days at 400°C and $P_{\text{O}_2} = 2.1$ atm, and then rapidly quenching them to room temperature. Magnetic susceptibility measurements did not detect the presence of second phases, and X-ray diffraction showed well ordered bulk structures, with the typical superstructure seen in Bi2201 and Bi2212. Optimally doped Bi2212 ($T_c = 90$ K) and Bi2201 ($T_c = 34$ K) with $\Delta T_c(10\% - 90\%) = 1$ K were also studied for comparison. ARPES experiments were performed at the Stanford Synchrotron Radiation Laboratory (SSRL) on a beamline equipped with a Scienta SES200 electron analyzer. Multiple ARPES spectra were acquired simultaneously in a narrow window of $0.5^\circ \times 14^\circ$ with, unless otherwise specified, an angular resolution of 0.3° (along the cut direction) and an energy resolution of 10 meV. The samples were aligned by Laue diffraction, and cleaved *in-situ* under a pressure better than 5×10^{-11} torr. Bi2223 samples #1, #3 (#2, #4) were cleaved at $T = 10$ K ($T = 125$ K).

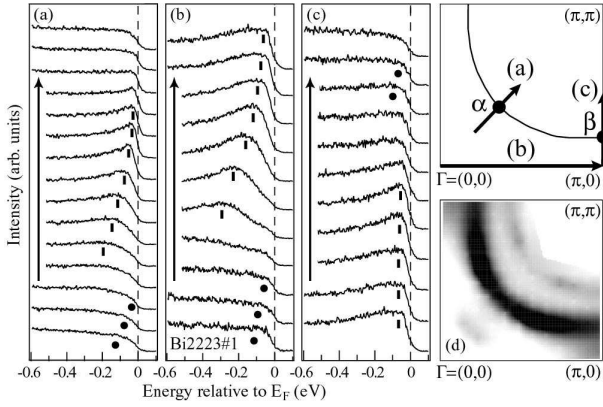


FIG. 1. (a-c) Normal state Bi2223 ARPES spectra along the high-symmetry lines, as indicated in the BZ sketch (data taken at 125 K with 21.2 eV photons and angular resolution of 0.24° , 0.6° , and 0.3° , respectively). Main (*umklapp*) bands are marked with bars (circles). (d) Integrated E_F -intensity map (± 10 meV) symmetrized with respect to $(0,0)$ - (π,π) .

Data were collected within 12 hours after cleaving and aging effects were negligible.

Fig. 1 presents the normal state ARPES spectra measured on Bi2223 along the high symmetry directions of the first Brillouin zone (BZ). Similar to what has been observed on optimally doped Bi2201 and Bi2212 [3], the quasiparticle band is rather flat near $(\pi,0)$ while it is quite dispersive and defines a clear Fermi crossing along the $(0,0)$ - (π,π) direction. The *umklapp* bands, one of the characteristics of the Bi-family of cuprates, are also detected. The Fermi surface (FS) can be identified by the local maxima of the intensity map obtained by integrating the ARPES spectra within a narrow energy window at the Fermi energy (E_F), after the spectra were normalized with respect to the high energy spectral weight. As in the case of Bi2201 and Bi2212 [3], one main and two weak *umklapp* FSs, shifted by $\pm(0.21\pi, 0.21\pi)$ with respect to the main FS, are clearly observed (Fig. 1d).

By tracking the energy position of the leading-edge midpoint (LEM) as a function of temperature and momentum, one can identify an anisotropic pseudogap and a superconducting gap (Δ) consistent with a *d*-wave symmetry. Figs. 2a and 2b show that at α , where the FS crossing along the nodal region is found (see the BZ sketch in Fig. 1), the LEMs of both normal and superconducting state spectra are located at E_F , indicating the absence of any gap. On the other hand, in the antinodal region (i.e., at β) the LEM is always shifted below E_F , corresponding to an 11 meV pseudogap above T_c and a 33 meV superconducting gap below T_c . The momentum dependence of both normal and superconducting state gaps along the normal state FS is summarized in Fig. 2c. The superconducting gap can be fitted to the *d*-wave functional form $\Delta = \Delta_0 |\cos k_x - \cos k_y|/2$ (where Δ_0 is the superconducting gap amplitude), while the pseudogap vanishes in wide momentum-space regions resulting in a partially gapped FS (or, equivalently, four discon-

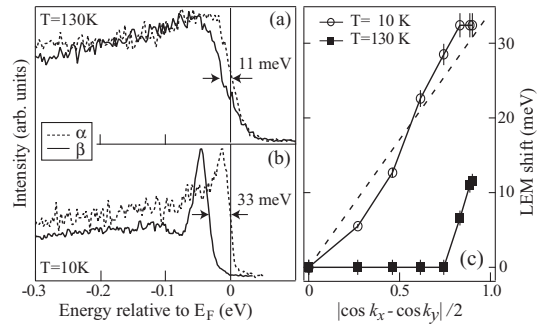


FIG. 2. (a) Normal and (b) superconducting state Bi2223 spectra measured with 21.2 eV photons at α and β (see BZ sketch in Fig. 1). (c) Position of the leading-edge midpoint (LEM) above and below T_c along the normal state FS. The dashed line is a fit to the *d*-wave gap functional form.

nected FS arcs in the BZ) at 130 K. Similar phenomena have also been observed in Bi2212 [4]. Furthermore, for the Bi2223 samples #2-4 the pseudogap at β was found to vary from 6 to 9 meV at 125 K (which is possibly caused by some small variations in carrier dopings), and the sample with larger pseudogap also has a larger superconducting gap.

Again in analogy with the case of Bi2212 [5], in Fig. 2 one also notices that the normal state spectrum at α sharpens up upon entering the superconducting state, but the most dramatic change in the lineshape takes place at β , where the spectrum evolves into a *peak-dip-hump* structure below T_c . This so-called superconducting peak, which dominates the spectral function in the $(\pi,0)$ region, has been argued to be an important characteristics of the HTSCs [6]. It has so far been detected by ARPES only on Bi2212 [7] and Y123 [8], and the present results substantiate its existence in the spectral function of an $n=3$ system. In order to gain more information, detailed temperature dependence measurements were performed at $(\pi,0)$, and the results are presented in Fig. 3a. The superconducting peak emerges slightly above T_c (i.e., at 116 K). Upon further cooling the sample below T_c , its intensity increases rapidly before it eventually saturates at low temperatures, while the total spectral weight is conserved (within 1-2%). At the same time, the LEM shifts to high binding energies reflecting the opening of the superconducting gap (Fig. 3b). Note also that, due to the weak quasiparticle dispersion in the flat band region, the spectra at $(\pi,0)$ and β exhibit a very similar behavior, as emphasized by Fig. 3b.

So far, we have shown that various properties of Bi2223 qualitatively resemble those of Bi2212 and/or Bi2201. The natural question is: what part of the electronic structure of Bi2223 can account for the highest T_c among the Bi-family of cuprates? To further investigate this issue, we compare in Fig. 4a the superconducting state $(\pi,0)$ spectra from optimally doped Bi2201 and Bi2212, and nearly optimally doped Bi2223 taken under the same experimental conditions (except for the higher energy res-

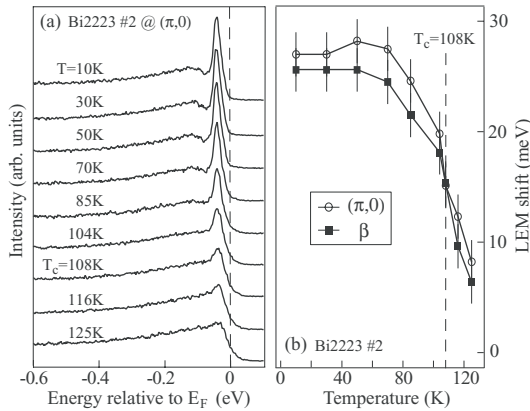


FIG. 3. (a) Temperature dependence of the Bi2223 $(\pi, 0)$ spectra and (b) of the LEM energy shift at $(\pi, 0)$ and β .

olution, i.e. 6meV, used for the Bi2201 data). The superconducting gap magnitude Δ_0 can be estimated by either the position of the superconducting peak or the LEM shift below E_F in the $(\pi, 0)$ spectra. We found that the average LEM (peak position) gap values are 10 (21), 24 (40), 30 (45) meV for the $n = 1, 2, 3$ systems, respectively. As shown in Fig. 4b, the gap value of the three different systems scales linearly with the corresponding T_c . In particular, the LEM gap can be well fitted by a line across the origin corresponding to an n -independent ratio $2\Delta_0/k_B T_c \simeq 5.5$. Furthermore, from ARPES and tunnelling spectroscopy results reported for other families of cuprates it is found that the values of Δ_0 for optimally doped LSCO [9], Bi2212 [10], YBCO [8,11], and Hg1212 [12] follow the same gap versus T_c linear relation (see Fig. 4b).

From the data presented in Fig. 4a, one can also extract the so-called superconducting peak ratio (SPR), which is defined as the ratio between the integrated spectral weight of the superconducting peak and that of the whole spectrum (i.e., from -0.5 to $+0.1$ eV). As shown in Fig. 4a, for the Bi2223 sample #2, the peak intensity is obtained by fitting the smooth “background” with a phenomenological function and then subtracting its contribution to the total integrated weight, as discussed in detail elsewhere [13]. For Bi2201, the superconducting peak is not resolved in the ARPES data and therefore its SPR is estimated to be close to zero. In recent scanning tunnelling spectroscopy (STS) experiments a superconducting peak in the density of state was observed for Bi2201. This, however, was detected only at certain locations on the cleaved sample surface and was not resolved in the spatially averaged STS spectra [14], consistent with what is observed by ARPES. For Bi2212 and Bi2223, the spectra in Fig. 4a (normalized at high binding energy to allow a direct comparison) indicate that the superconducting peak amplitude for Bi2223 is much larger than that of Bi2212. Overall, the SPRs of these systems scale linearly with T_c (Fig. 4c) [15]. For Bi2212, it has been argued that the SPR is related to the phase stiffness of the condensate or superfluid density (ρ_s) [13,16].

The weak superconducting peak in the (spatially averaged) ARPES spectra from Bi2201 may then reflect a low superfluid density, and in fact the peak amplitude is negligible also in Bi2212 samples with $T_c < 50$ K [13]. The n -dependence of the SPR is qualitatively consistent with the muon spin resonance (μ SR) results, which show that ρ_s for the optimally doped cuprates increases with n (for $n \leq 3$), and scales with T_c in approximately a linear fashion as in the celebrated “Uemura plot” [17]. Therefore, the ARPES results together with those from tunnelling and μ SR indicate that both Δ_0 and ρ_s increase with T_c for the different optimally doped cuprates.

Within current understanding, Δ_0 and ρ_s are the two most important quantities in characterizing the superconducting state, as they reflect the strength of the two basic ingredients of superconductivity: pairing and phase coherence. T_Δ , the temperature at which the Cooper pairs start to form, is determined by pairing strength (or Δ_0); T_Σ , the temperature at which the Cooper pairs, if any, become phase coherent, is determined by the phase stiffness (or ρ_s). The superconducting phase transition temperature is given by $T_c = \min(T_\Delta, T_\Sigma)$ [18]. For conventional superconductors, $T_\Sigma \gg T_\Delta$; therefore, $T_c = T_\Delta$ and phase fluctuations are not important in determining T_c . The situation is different for the HTSCs: in order to have high T_c , it is necessary to have both large Δ_0 and ρ_s , as we have seen for nearly optimally doped Bi2223. The reason for this is that HTSCs are doped Mott insulators with low carrier density, for which T_Σ and T_Δ are comparable and proposed to have the doping dependence sketched in Fig. 5 [18,19]. The crossing of $T_\Delta(x)$ (x being doping) and $T_\Sigma(x)$ gives $T_\Delta(x_{opt}) = T_\Sigma(x_{opt}) = T_{c,opt}$

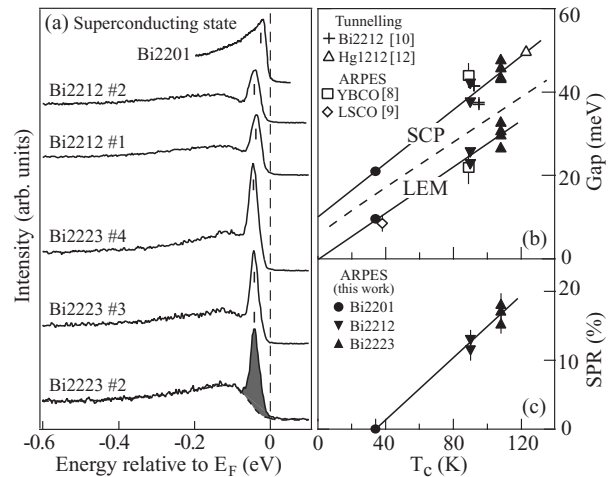


FIG. 4. (a) Superconducting state $(\pi, 0)$ spectra measured at 10 K with 22.7 eV photons on optimally doped Bi2201 and Bi2212, and nearly optimally doped Bi2223. (b) Superconducting gap magnitude as estimated from the position of the superconducting peak (SCP) and the LEM shift (separated by the dashed line), for various optimally doped materials, and (c) superconducting peak ratio (SPR) extracted from the data in (a), plotted versus T_c .

(with the subscript *opt* referring to optimal doping, which is found to be approximately fixed at $x_{opt} \simeq 0.16$ for many HTSCs [20]). The approximate linear relations $\Delta_{0,opt} \propto T_{c,opt}$ and $\rho_{s,opt} \propto T_{c,opt}$ observed for various optimally doped systems lead to $T_{\Sigma}(x_{opt}) \propto \rho_{s,opt}$ and $T_{\Delta}(x_{opt}) \propto \Delta_{opt}$, as theoretically proposed [18].

We have shown that many aspects of the electronic structure of Bi2223, such as the Fermi surface topology and flat band dispersion, resemble those of Bi2212 and Bi2201. A preliminary lineshape analysis [21] suggests that the interlayer coupling between CuO₂ planes within a multilayer block is not stronger, but possibly even weaker in Bi2223 than in Bi2212, where bilayer band splitting, which causes multiple features or broader lineshapes in ARPES spectra, were recently observed [22]. This and the fact that $T_{c,opt}$ in Hg1201 is comparable to that of Bi2212 indicate that the interlayer coupling within a multilayer block is not the dominant factor for the enhancement of T_c . Moreover, $T_{c,opt}$ does not scale with n in a linear way within a specific HTSC family; and for a given n , e.g. $n = 1$, $T_{c,opt}$ varies from 30 K to 100 K for different families of cuprates. Instead, we have shown that $T_{c,opt}$ scales approximately linearly with both $\rho_{s,opt}$ and $\Delta_{0,opt}$. One could speculate that the resolution of the T_c vs. n problem might be incorporated into a broader task, namely the search for the parameters that enhance both superconducting gap and superfluid density, and in turn the optimal T_c . These parameters could be affected by n and other conspiring factors, for which various candidates have already been proposed, including superconductivity enhancement in the non-CuO₂ layers [23], or as a consequence of impurities and distortion/strain introduced into the system [24,25]. To highlight these unknown parameters, we add a third axis to the phase diagram of the hole-doped HTSCs (Fig. 5), along which both pairing strength and phase stiffness (and thus $T_{c,opt}$) increase with the same monotonic trend, contrary to their opposite trends along the doping axis. In this way, the Bi-based cuprates and possibly different families of HTSCs can be integrated into one comprehensive phase diagram.

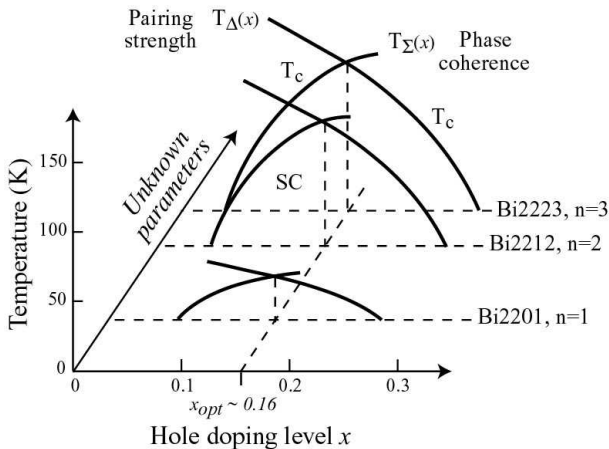


FIG. 5. Qualitative phase-diagram for the Bi-based HTSCs.

Acknowledgements: DLF and ZXS would like to thank S. Maekawa and T. H. Geballe for helpful discussions. SSRL is operated by the DOE Office of Basic Energy Science Divisions of Chemical Sciences and Material Sciences. The Stanford experiments are also supported by the NSF grant DMR0071897 and ONR grant N00014-98-1-0195-A00002. The crystal growth work at Stanford was supported by DOE under Contract Nos. DE-FG03-99ER45773-A001 and DE-AC03-76SF00515. MG is also supported by the A. P. Sloan Foundation and NSF CAREER Award No. DMR-9985067.

- [1] M. Di Stasio, K.A. Muller, and L. Pietronero, Phys. Rev. Lett. **64**, 2827 (1990), and references therein.
- [2] J.M. Tarascon *et al.*, Phys. Rev. B **38**, 8885 (1992).
- [3] Z.-X. Shen and D.S. Dessau, Phys. Rep. **253**, 1 (1995); A. Damascelli, D.H. Lu, and Z.-X. Shen, J. Electron Spectrosc. Relat. Phenom. **117-118**, 165 (2001); D.W. Lynch and C.G. Olson, *Photoemission Studies of High-Temperature Superconductors* (Cambridge University Press, 1999).
- [4] D.S. Marshall *et al.*, Phys. Rev. Lett. **76**, 4841 (1996); M. Norman *et al.*, Nature **392**, 157 (1998).
- [5] A. Kaminski *et al.*, Phys. Rev. Lett. **84**, 1788 (2000).
- [6] See for example D.-H. Lee, Phys. Rev. Lett. **84**, 2694 (2000); T. Senthil and M.P.A. Fisher cond-mat/9910224; E.W. Carlson *et al.*, Phys. Rev. B **62**, 3422 (2000).
- [7] D.S. Dessau *et al.*, Phys. Rev. Lett. **66**, 2160 (1991).
- [8] D.H. Lu *et al.*, Phys. Rev. Lett. **86**, 4370 (2001).
- [9] X.J. Zhou *et al.*, unpublished.
- [10] Ch. Renner *et al.*, Phys. Rev. Lett. **80**, 149 (1998); Y. De Wilde *et al.*, *ibid.* 153 (1998); N. Miyakawa *et al.*, *ibid.* 157 (1998).
- [11] For YBCO, because of the additional gap anisotropy due to the presence of the CuO chains [8], the maximum gap amplitude (i.e., Δ_0 at the Y point) is plotted in Fig.4b.
- [12] J.Y.T. Wei *et al.*, Phys. Rev. B **57**, 3650 (1998).
- [13] D.L. Feng *et al.*, Science **289**, 277 (2000).
- [14] M. Kugler *et al.*, Phys. Rev. Lett. **86**, 4911 (2001).
- [15] We note that Bi2223 and Bi2212 have different structures and thus possibly different photoemission matrix elements. However, the large enhancement of the superconducting peak in Bi2223 and the qualitative aspect of Fig. 4c are not likely just matrix element artifacts.
- [16] H. Ding *et al.*, cond-mat/0006143.
- [17] Y.J. Uemura *et al.*, Nature **364**, 605 (1993), and references therein.
- [18] V.J. Emery and S. Kivelson, Nature **374**, 434 (1995).
- [19] Y.J. Uemura, Physica C **282-287**, 194 (1997), which also shows that ρ_s (and thus T_{Δ}) eventually decreases in the overdoped regime. It is omitted here for simplicity, and will not affect the qualitative conclusions drawn here.
- [20] M.R. Presland *et al.*, Physica C **176**, 95 (1991); J. Tallon *et al.*, Phys. Rev. B **51**, 12911 (1995); S. Ono *et al.*, Phys. Rev. Lett. **85**, 638 (2000).
- [21] D.L. Feng, Ph.D. thesis, Stanford University, 2001.
- [22] D.L. Feng *et al.*, Phys. Rev. Lett. **86**, 5550 (2001); *ibid.*, cond-mat/0107073; Y.-D. Chuang *et al.*, cond-mat/0102386; *ibid.*, 0107002.
- [23] T.H. Geballe and B.Y. Mozyshes, Physica C **341-348**, 1821 (2000).

- [24] H. Eisaki *et al.*, unpublished.
- [25] A. Bianconi *et al.*, Int. J. Mod. Phys. B **14**, 3342 (2000).